Journal of Experimental Botany, Vol. 61, No. 9, pp. 2433–2445, 2010
doi:10.1093/jxb/erq075 Advance Access publication 16 April, 2010
This paper is available online free of all access charges (see http://jxb.oxfordjournals.org/open_access.html for further details)

Journal of Experimental Botany
www.jxb.oxfordjournals.org

RESEARCH PAPER

Comparative transcriptome analysis of green/white variegated sectors in *Arabidopsis yellow variegated2*: responses to oxidative and other stresses in white sectors

Eiko Miura, Yusuke Kato and Wataru Sakamoto*

Research Institute for Bioresources, Okayama University, Kurashiki, Okayama 710-0046, Japan

* To whom correspondence should be sent: E-mail: saka@rib.okayama-u.ac.jp

Received 22 January 2010; Revised 5 March 2010; Accepted 8 March 2010

Abstract

The *yellow variegated2* (*var2*) mutant in *Arabidopsis thaliana* has been studied as a typical leaf-variegated mutant whose defect results from the lack of FtsH2 metalloprotease in chloroplasts. The *var2* green sectors suffer from photo-oxidative stress and accumulate high levels of reactive oxygen species (ROS) because of compromised Photosystem II repair. This study investigated and compared microarray-based expression profiles of green and white sectors of *var2* leaves. Results suggest that ROS that accumulate in chloroplasts of *var2* green sectors do not cause much significant change in the transcriptional profile related to ROS signalling and scavenging. By contrast, transcriptome in the white sectors apparently differs from those in the green sectors and wild type. Numerous genes related to photosynthesis and chloroplast functions were repressed in the white sectors. Furthermore, many genes related to oxidative stress were up-regulated. Among them, ROS scavenging genes were specifically examined, such as *Cu/Zn superoxide dismutase 2* (*CSD2*), that were apparently up-regulated in white but not in the green sectors. Up-regulation of CSD2 appears to be partly attributable to the lack of a microRNA (*miR398*) in the white sectors. It was concluded that the white sectors exhibit a response to oxidative and other stresses, including CSD2 up-regulation, which might be commonly found in tissues with abnormal chloroplast differentiation.

Key words: *Arabidopsis*, chloroplasts, *miR398*, plastids, reactive oxygen species (ROS), superoxide dismutase (SOD), *yellow variegated2* (*var2*).

Introduction

Leaf variegation is a common phenomenon in many ornamental plants and crops. Mutations in both nuclear and organelle genomes reportedly cause leaf variegation or striping (Von Wirén *et al.*, 1994; Sakamoto, 2003; Yaronskaya *et al.*, 2003). Although molecular characterization of leaf-variegated mutants has confirmed that leaf variegation results from various redundant functions related to chloroplasts, the precise mechanism leading to such chimeric chloroplast development in the same leaf tissues remains poorly understood. Generation of non-identical variegated sectors in each leaf suggests a threshold level of factor(s) that arrest proplastid differentiation into chloroplasts. Consequently, close examination of the formation of variegated tissues through various experimental approaches enables us to understand important factors affecting chloroplast development.

The variegated mutant *yellow variegated2* (*var2*) in *Arabidopsis thaliana* has been specifically investigated as a model to study the formation of green/white variegated sectors. True leaves in *var2* form non-identical variegated sectors, indicating that chloroplast differentiation is defective at an early phase of leaf cell lineage (Sakamoto *et al.*, 2009). The *VAR2* locus encodes FtsH2, an isoform of chloroplastic metalloprotease FtsHs (Chen *et al.*, 2000; Takechi *et al.*, 2000). In chloroplasts, FtsH plays an essential role in the progressive degradation of thylakoid membrane proteins along with other proteases (Adam *et al.*, 2006; Sakamoto, 2006; Kato and Sakamoto, 2009).

Chloroplast FtsH, which forms a hetero-complex, comprises four major isomers (FtsH1, 2, 5, 8), which are functionally distinguished as two types (FtsH1 and FtsH5 belong to Type A; FtsH2 and FtsH8 belong to Type B) (Zaltsman *et al.*, 2005). Because FtsH levels are regulated on a post-translational level, a lack of FtsH2 results in an overall decrease in the FtsH heteromeric complex (Sakamoto *et al.*, 2003; Yu *et al.*, 2008). It was assumed that a level of FtsH2 below the threshold caused leaf variegation (Miura *et al.*, 2007; Yu *et al.*, 2008). Similarly to *var2*, a lack of FtsH5 results in an additional variegated mutant known as *yellow variegated1* (*var1*) (Sakamoto *et al.*, 2002). Based on these phenotypes in *var1* and *var2*, it is proposed that FtsH is involved in both thylakoid formation and protein degradation.

Aside from the variegation phenotype in the mutant, FtsH protease was also shown to participate in the specific degradation of D1 protein in the Photosystem II (PSII) reaction centre as a critical component of the PSII repair cycle (Bailey *et al.*, 2002; Nixon *et al.*, 2005; Kato *et al.*, 2009). Lack of FtsH in *var1* and *var2* mutant leaves show impaired D1 degradation when exposed to photoinhibitory light conditions (Bailey *et al.*, 2002; Sakamoto *et al.*, 2002; Miura *et al.*, 2007). More importantly, it was found that chloroplasts in *var2* green sectors accumulate substantial levels of reactive oxygen species (ROS) (Kato *et al.*, 2007). It was assumed that such an elevated ROS reflects gene expression in *var2* green sectors.

In this study, a comparative microarray analysis was performed between wild-type ecotype Columbia (Col) leaves and green and white sectors in *var2*. Chloroplast ROS in *var2* green sectors do not appear to induce ROS signalling pathway-related genes and ROS-scavenging genes. By contrast, a considerable number of transcripts were shown to increase or decrease in *var2* white sectors. It is particularly interesting that one-quarter of the increased genes correlated with response to stresses, especially to oxidative stress. Among the up-regulated genes, particular attention was devoted to Cu/Zn superoxide dismutase (SOD), which catalyses the oxidation of superoxide radicals (O_2^-) into hydrogen peroxide (H_2O_2) in chloroplasts (Asada, 2006). In *var2*, the Cu/Zn SOD levels do not coincide with intra-chloroplastic ROS, but are instead increased in a white sector-specific manner. These results imply that variegated sectors might be maintained positively through the expression of specific genes related to oxidative stress.

Materials and methods

Plant materials and growth conditions

Wild-type *Arabidopsis thaliana* Columbia (Col) ecotype and the *var2-1* (*var2*) mutant were used as previously described (Takechi *et al.*, 2000) and grown in MS medium supplemented with Gamborg's vitamins (Sigma–Aldrich Corporation). Four-week-old *Arabidopsis* plants grown in standard MS medium were used for all experiments unless otherwise noted. The MS medium supplemented with 1.5% (w/v) sucrose and 0.7% (w/v) agar is hereafter designated as standard MS medium. Plants were maintained under a 12 h light (70 μmol m^{-2} s^{-1})/12 h dark cycle at 22 °C. For making a copper sufficient condition, 5 μM $CuSO_4$ was added to standard MS medium.

Microarray experiment

A microarray experiment was performed using a custom service offered by Hokkaido System Science Co. Ltd. (Sapporo, Japan). Total RNA from three biological replicates of each sample was extracted. Then cDNA was synthesized from RNA samples; the cRNA was subsequently labelled with Cyanin3 using the Quick Amp Labelling Kit (Agilent Technologies Inc.). The cRNA target solution was prepared after labelled cRNA was purified using RNeasy mini spin columns (Qiagen Inc.). The cRNA target solution was then applied to the microarray (*Arabidopsis* Oligo DNA microarray ver. 4.0; Agilent Technologies Inc.) and hybridization was performed. After washing and air-drying of the microarray, the slide was scanned at a resolution of 5 μm using a microarray scanner (Agilent Technologies Inc.). Digitalized data of the scanning were imported into software (GeneSpring GX 10; Agilent Technologies Inc.) and normalized to shift to the 75 percentile. The following flagged features were cut off: features that were not positive and significant, and features that were not above background levels. After filtering for flags, 32 348 probes remained. On the microarray, some genes are represented as several oligonucleotides that have distinct 60-mer sequences from different regions within the same genes. For metabolic pathway analysis, the normalized signal values (per chip: normalized to the 75th percentile) were transformed to $\log_{10}$ values. Values averaged from three biological replicates were presented on the pathway maps through KaPPA-View (Tokimatsu *et al.*, 2005) according to the manual provided on the web site (http://kpv.kazusa.or.jp/kappa-view/). The microarray data were deposited to GEO (Accession no. GSE18646).

RNA extraction, RT-PCR and real-time RT-PCR analysis

Total RNAs were extracted from leaves (RNeasy Plant Mini Kit; Qiagen Inc.). Then RT-PCR was performed (Qiagen One Step RT-PCR Kit; Qiagen Inc.). Quantitative RT-PCR was conducted (LightCycler; Roche Diagnostics Corp.) according to the manufacturer's recommendations. For real-time RT-PCR analysis, a kit (TaKaRa One Step SYBR PrimeScript RT-PCR Kit; Takara) was used. Briefly, 2 ng of total RNA was used as template; then RT-PCR was run using the following conditions: 1 cycle of 30 min at 50 °C, 10 s at 95 °C, and 50 cycles of 5 s at 95 °C, 10 s at 57 °C, and 10 s at 72 °C. Then *ACTIN* was used as an internal control. Software (LightCycler Software Version 4.0; Roche Diagnostics Corp.) was used to quantify each transcript level. Real-time RT-PCR reactions were performed as three technical and three biological replicates. Primers used for RT-PCR and real-time RT-PCR are listed in Supplementary Table S2 at JXB online.

Immunoblot analysis

Leaves from Col and *var2* were homogenized in extraction buffer (50 mM HEPES, 5 mM EDTA, and 10 mM β-mercaptoethanol). Samples for SDS-PAGE were diluted with an equal volume of 2× sample buffer [125 mM TRIS (pH 6.8), 10% (w/v) sucrose, 4% (w/v) SDS, 10% (v/v) β-mercaptoethanol, and 0.004% (w/v) bromophenol blue]. Samples were normalized to fresh weight, separated on 12% SDS polyacrylamide gels and transferred to polyvinylidene difluoride membranes (Atto Corp.) by electroblotting. Blocking, incubation with antibodies, and detection were performed using a Western blot detection system (ECL Plus advance; GE Healthcare). Then CSD1 was detected using the CSD2 antibody as a result of its ability to cross-react with the CSD1 protein (Abdel-Ghany and Pilon, 2008).

SOD activity

Total SOD activity was assayed for its ability to inhibit the photochemical reduction of NBT. Leaves (30 mg) were homogenized in extraction buffer [50 mM HEPES-KOH (pH 7.2), 5 mM EDTA, 20% (v/v) glycerol and 0.05% (w/v) bromophenol blue]. Cooled samples were separated in 15% native PAGE gels in the absence of SDS at 4 °C. After electrophoresis, the gel was incubated with 1 mg ml^{-1} NBT (Sigma-Aldrich Corp.) for 30 min in the dark. The gel was subsequently transferred to a solution [0.1 M potassium phosphate buffer (pH 7.0), 0.028 mM riboflavin, and 28 mM TEMED] and incubated for 20 min in the dark. After incubation, the gel was exposed under light conditions until bands were apparent.

Northern blot analysis

Total RNA (20 μg) suspended in H_2O was mixed with an equal volume of 2× formamide loading buffer [16% (v/v) formaldehyde, 50% (v/v) deionized formamide, 20% (v/v) glycerol, and 0.05% (w/v) bromophenol blue] and heated at 95 °C for 5 min. After loading the RNA samples on a 15% 6 M urea polyacrylamide gel using 0.5×TBE buffer [89 mM TRIS base, 89 mM boric acid, 1 mM EDTA (pH 7.0)] as running buffer, the gel was stained with ethidium bromide (EtBr) for 5 min. The gel was then rinsed to remove excess EtBr and transferred to a Hybond-N^+ nylon membrane (GE Healthcare) by capillary transfer with 20× SSC buffer. The blotted membrane was rinsed with 20× SSC buffer and UV-crosslinked for 2 min. The membrane was subsequently soaked in FPH solution [0.5 M sodium phosphate (pH 7.2), 7% (w/v) SDS, 1 mM EDTA (pH 7.0)] in a hybridization bag and incubated at 40 °C for 30 min. During pre-hybridization, oligonucleotides complementary to *miR398 b & c* and *small nuclear RNA U6* (*U6 snRNA*) were end-labelled with [γ-^{32}P]ATP using T4 polynucleotide kinase (Takara Bio Inc.). For this study, DNA oligonucleotide probes specific for *miR398 b & c* (5′-CAGGGGTGACCTGAGAACACA-3′) and *U6 snRNA* (5′-TCATCCTTGCGCAGGGGCCA-3′) were used. After removing unincorporated radionucleotide with Microspin G-25 columns (GE Healthcare), labelled probes were added to the FPH solution and hybridized at 40 °C for 2 h. After hybridization, the membrane was washed twice for 10 min in 2× SSC+0.1% SDS and once for 20 min in 0.2× SSC+0.1% SDS. The membrane was covered in plastic wrap and placed on an imaging plate (Fuji Photo Film Co. Ltd.) for 5 d. Radiolabels were detected with a BAS 1000 image analyser (Fuji Photo Film Co. Ltd.).

Results

Microarray and scatter plot analysis

To monitor transcriptional profiles in variegated leaves, DNA microarray analysis was conducted. Total RNA was extracted from micro-dissected green and white sectors from 4-week-old true leaves grown in standard MS medium under normal light intensity (70 μmol m^{-2} s^{-1}). Total RNA was also extracted from Col wild-type leaves and all reverse-transcribed RNAs were hybridized to the Agilent *Arabidopsis* ver. 4 DNA chip (n=3). ROS accumulation was monitored histochemically in our leaf materials for RNA extraction as reported previously and it was confirmed that *var2* green sectors significantly accumulate ROS (Fig. 1). The microarray contained a total of 43 663 oligonucleotide probes representing approximately 28 169 unique genes. All probes (43 663) on the array were filtered based on their flag values (see Materials and methods). A one-way ANOVA

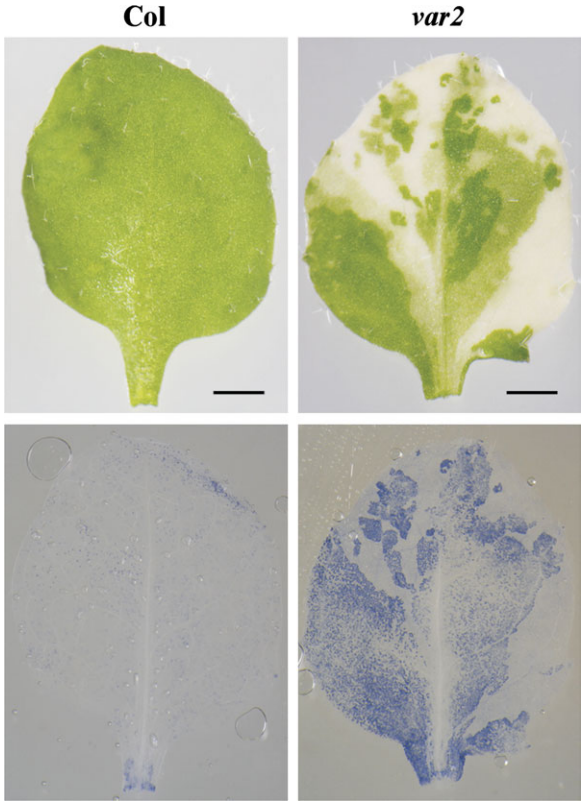

Fig. 1. ROS accumulation in *var2* green sectors. *In situ* detection of O_2^- by staining with NBT (blue, bottom panels) in 4-week-old wild-type Col and *var2* leaves. Bars=1 mm.

statistical test was performed using the Benjamini and Hochberg false discovery rate (BH-FDR) multiple testing correction (corrected P value <0.05) using software (GeneSpring GX 10; Agilent Technologies Inc.). Using this method, 9249 probes were chosen for further analyses described below.

A scatter plot analysis was performed first. Accumulation of transcripts corresponding to each gene, represented as a normalized signal value (Log_2), was shown between two of the three RNA samples. Comparison between Col and *var2* green sectors showed that most genes fit within a 2-fold difference (Fig. 2), indicating that the transcriptional profile is similar between *var2* green sectors and Col. In stark contrast, a comparison between Col and *var2* white sectors showed that numerous genes were beyond the 2-fold difference and showed either an increase or a decrease in the white sectors (Fig. 2; see Supplementary Fig. S1 at *JXB* online). The same trend was also true between *var2* green and white sectors because Col and *var2* green sectors showed a similar expression profile. These results demonstrated that many genes are responsive to the formation of white sectors at the transcription level.

Categories of up- and down-regulated genes as revealed by gene ontology analysis

To compare differential transcriptomes in detail in variegated tissues, genes were characterized for which transcripts

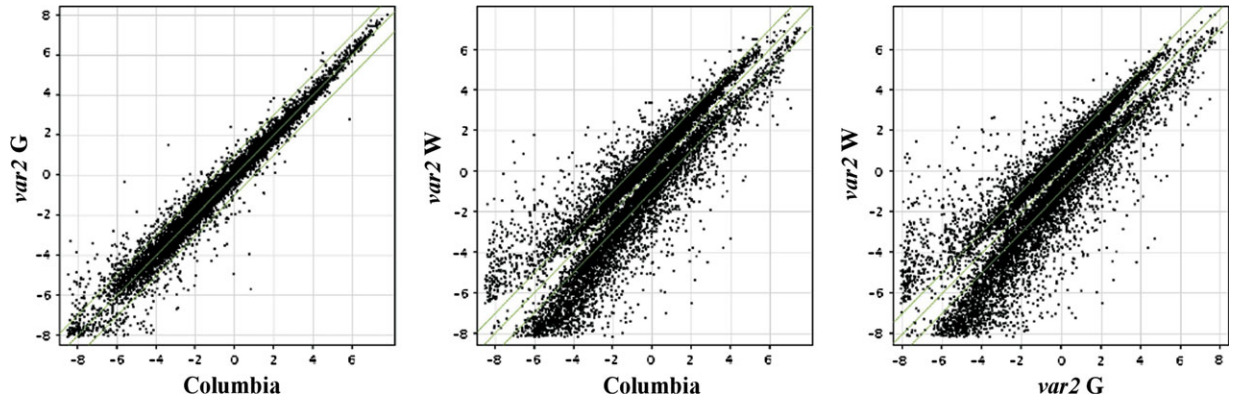

Fig. 2. Scatter plot analysis. Normalized signal values (Log_2) were normalized from Columbia, *var2* green sectors (*var2* G) and *var2* white sectors (*var2* W). Each gene is represented as one dot. Green lines represent the 2-fold change cutoff.

accumulated differentially between the green and white sectors in *var2*. When a cutoff was made by a 2-fold change, 1304 probes were selected as up-regulated and 3194 probes as down-regulated (see Supplementary Fig. S1 at *JXB* online). To classify these genes based on function, a subsequent gene ontology (GO) analysis was performed according to the method described by Ashburner *et al.* (2000). In this method, genes were initially categorized into three primary ontologies (molecular function, biological process, and cellular component), based on 'GO terms' assigned to each gene. The selected genes were further categorized by hierarchic functional categories and GO categories containing up- or down-regulated genes at the significant level (hypergeometric test, Benjamini–Yekutieli (BY)-corrected *P*-value <0.1) were selected. 80 down- and 27 up-regulated GO categories were detected; they are listed, respectively, in Tables 1 and 2.

Among the down-regulated categories, 17 GO categories (21.25%) were identified that were related to either chloroplasts or photosynthesis (Fig. 3A). Three representative categories (Photosynthesis, Light-harvesting complex, and Tetrapyrrole binding) are presented as heat maps in Fig. 3B–D. The white sectors appeared to lack gene products from these three categories because plastids in the white sectors are devoid of thylakoid membranes. A loss of light-harvesting complex II (LHCII) in the white sectors was consistent with our previous result (Kato *et al.*, 2007). Other down-regulated GO categories related to chloroplast biogenesis included Thylakoid, Thylakoid membranes, Plastoglobule, Photosystem, Photosystem I, and Chlorophyll binding (Table 1). These data suggest that the arrest of differentiation from proplastids into chloroplasts partially results from an irreversible repression of these photosynthetic genes.

Regarding up-regulated categories, all GO categories were principally unrelated to photosynthesis and appeared to converge to two major classes (Table 2). One category was related to RNA metabolism (9 GO categories: 30%). The other was related to several stresses (7 GO categories: 25.92%) (Fig. 3A). Examples of the stress-related GO categories are shown as heat maps in Fig. 3E–I. It is notable that many of these stresses are related to oxidative stress and ROS (Table 2). Therefore, it is considered that the white sectors are highly susceptible to oxidative damage because of impaired plastid development.

Metabolic pathway analysis between Col and var2 *green sector*

As implied in our scatter plot analysis, transcriptional profiles between Col and *var2* green sectors are similar. Indeed, no GO category was detected that was significantly different between these two samples. It is therefore suggested that *var2* green sectors do not respond strongly to photo-oxidative stress and ROS. To investigate further whether any cellular function exists that is not detected by our GO analysis, but which is affected in *var2* green sectors, a metabolic pathway analysis was performed in which quantitative changes in individual transcripts were compared using software (KaPPA-View 2; http://kpv.kazusa.or.jp/kappa-view/). Comparison of 166 pathways between Col and *var2* green sectors showed differences in only one pathway: 'starch biosynthesis' (see Supplementary Fig. S2 available at *JXB* online). Altered starch metabolism was also reported using a similar pathway analysis in the green sector of another variegated mutant *immutans* (*im*) (Aluru *et al.*, 2007, 2009). It is possible that green sectors act partly as a source tissue and that they need to transport more sugar into white sectors than normal green leaves.

Elevated expression of ROS scavenging enzymes in white sectors

It was initially assumed that genes corresponding to ROS scavenging enzymes such as SOD and ascorbate peroxidase (APX) are up-regulated in *var2* because of the impaired PSII repair and photo-oxidative damage. Our results showed that although up-regulation occurred in some of the genes, it was contrary to our assumption: white sectors but not green sectors seem to have increased levels of ROS scavenging enzymes. To investigate such differential expression in this study, expression of SOD and APX, particularly of the plastid localized SOD and APX isoforms was examined further. In *Arabidopsis*, seven SODs had been

Table 1. Significantly enriched gene ontologies among down-regulated genes in *var2* white sectors compared to *var2* green sectors

Gene ontology (description and term)[a]	Raw *P*	BY-corrected *P*	Number[b]
Cellular component			
Anchored to membrane; GO:0031225	0.000	0.018	44/235
Cell surface; GO:0009986|GO:0009928|GO:0009929	0.000	0.018	7/13
Chloroplast part; GO:0044434	**0.000**	**0.041**	**54/443**
Chloroplast thylakoid membrane; GO:0009535	**0.000**	**0.000**	**53/250**
Chloroplast thylakoid; GO:0009534	**0.000**	**0.000**	**53/295**
Extracellular region; GO:0005576	0.000	0.023	21/245
Light-harvesting complex; GO:0030076	**0.000**	**0.000**	**16/25**
Microtubule associated complex; GO:0005875	0.000	0.001	20/64
Microtubule cytoskeleton; GO:0015630	0.000	0.030	20/132
Organelle subcompartment; GO:0031984	0.000	0.000	53/300
Photosynthetic membrane; GO:0034357	**0.000**	**0.000**	**55/319**
Photosystem I reaction center; GO:0009538	**0.000**	**0.002**	**7/8**
Photosystem I; GO:0009522	**0.000**	**0.000**	**9/15**
Photosystem; GO:0009521|GO:0030090	**0.000**	**0.000**	**9/42**
Plastid thylakoid membrane; GO:0055035	**0.000**	**0.000**	**53/250**
Plastid thylakoid; GO:0031976	**0.000**	**0.000**	**53/298**
Plastoglobule; GO:0010287	**0.000**	**0.003**	**19/58**
Thylakoid membrane; GO:0042651	**0.000**	**0.000**	**54/258**
Thylakoid part; GO:0044436	**0.000**	**0.000**	**54/301**
Thylakoid; GO:0009579	**0.000**	**0.000**	**55/315**
Biological process			
Biological regulation; GO:0065007	0.000	0.000	98/3188
Carbohydrate biosynthetic process; GO:0016051|GO:0006093	0.000	0.000	17/244
Carbohydrate metabolic process; GO:0005975	0.000	0.001	63/743
Carboxylic acid biosynthetic process; GO:0046394	0.000	0.001	20/148
Cell communication; GO:0007154	0.000	0.001	76/989
Cell surface receptor linked signal transduction; GO:0007166	0.000	0.002	35/154
Cell wall organization and biogenesis; GO:0007047	0.000	0.014	18/232
Cellular carbohydrate biosynthetic process; GO:0034637	0.000	0.000	10/167
Cellular carbohydrate metabolic process; GO:0044262|GO:0006092	0.000	0.000	11/363
Cytoskeleton-dependent intracellular transport; GO:0030705	0.000	0.014	18/70
DNA replication initiation; GO:0006270	0.000	0.046	7/11
DNA replication; GO:0006260	0.000	0.013	18/106
Enzyme linked receptor protein signalling pathway; GO:0007167	0.000	0.000	35/130
External encapsulating structure organization and biogenesis; GO:0045229	0.000	0.020	18/236
Fatty acid biosynthetic process; GO:0006633|GO:0000037	0.000	0.013	20/106
Glucosinolate biosynthetic process; GO:0019761	0.000	0.000	10/20
Glucosinolate metabolic process; GO:0019760	0.000	0.000	10/25
Glycoside biosynthetic process; GO:0016138	0.000	0.000	10/20
Glycoside metabolic process; GO:0016137	0.000	0.000	10/25
Glycosinolate biosynthetic process; GO:0019758	0.000	0.000	10/20
Glycosinolate metabolic process; GO:0019757	0.000	0.000	10/25
Jasmonic acid and ethylene-dependent systemic resistance; GO:0009861	0.000	0.096	11/34
Jasmonic acid biosynthetic process; GO:0009695	0.000	0.009	11/23
Jasmonic acid metabolic process; GO:0009694	0.000	0.009	11/23
Lipid metabolic process; GO:0006629	0.000	0.054	48/634
Microtubule-based movement; GO:0007018	0.000	0.002	18/52
Organic acid biosynthetic process; GO:0016053	0.000	0.001	20/148
Oxylipin biosynthetic process; GO:0031408	0.000	0.014	11/24
Oxylipin metabolic process; GO:0031407	0.000	0.014	11/24
Photosynthesis; GO:0015979	**0.000**	**0.000**	**25/102**
Plant-type cell wall loosening; GO:0009828	0.000	0.096	12/34
Plant-type cell wall modification; GO:0009827	0.000	0.069	13/38
Plant-type cell wall organization and biogenesis; GO:0009664	0.000	0.014	15/107

Table 1. *Continued*

Gene ontology (description and term)[a]	Raw *P*	BY-corrected *P*	Number[b]
Regulation of biological process; GO:0050789|GO:0050791	0.000	0.000	98/2947
Regulation of cell cycle; GO:0051726|GO:0000074	0.000	0.000	23/93
Regulation of cellular process; GO:0050794|GO:0051244	0.000	0.000	98/2814
Response to biotic stimulus; GO:0009607	0.000	0.037	27/425
Response to chemical stimulus; GO:0042221	0.000	0.000	3/1206
Response to endogenous stimulus; GO:0009719	0.000	0.000	2/706
Response to external stimulus; GO:0009605	0.000	0.000	27/250
Response to hormone stimulus; GO:0009725	0.000	0.003	2/645
Response to stimulus; GO:0050896|GO:0051869	0.000	0.000	63/2645
Response to wounding; GO:0009611|GO:0002245	0.000	0.002	27/114
Secondary metabolic process; GO:0019748	0.000	0.000	11/352
Signal transduction; GO:0007165	0.000	0.017	75/865
Transmembrane receptor protein tyrosine kinase signalling pathway; GO:0007169	0.000	0.000	35/130
Molecular function			
Catalytic activity; GO:0003824	0.000	0.000	121/7257
Chlorophyll binding; GO:0016168	**0.000**	**0.000**	**19/27**
Copper ion binding; GO:0005507	0.000	0.006	27/121
Cyclin-dependent protein kinase regulator activity; GO:0016538|GO:0003751|GO:0003752|GO:0003753	0.000	0.000	17/32
Enzyme regulator activity; GO:0030234	0.000	0.084	18/282
Hydrolase activity, acting on glycosyl bonds; GO:0016798	0.000	0.025	5/428
Kinase regulator activity; GO:0019207	0.000	0.000	17/40
Lyase activity; GO:0016829	0.000	0.014	10/324
Microtubule motor activity; GO:0003777	0.000	0.000	23/69
Molecular_function; GO:0003674|GO:0005554	0.000	0.097	866/23215
Motor activity; GO:0003774	0.000	0.002	25/90
Protein kinase regulator activity; GO:0019887	0.000	0.000	17/38
Protein serine/threonine kinase activity; GO:0004674	0.000	0.020	41/297
Tetrapyrrole binding; GO:0046906	**0.000**	**0.000**	**19/52**

[a] GO analysis was performed using a hypergeometric test with GeneSpring GX 10 software. Gene ontology categories are shown with significant Benjamini–Yekutieli FDR (BY–FDR)-corrected *P*-values <0.1. Gene categories related to photosynthesis and chloroplasts are shown as bold.
[b] Number indicates the number of genes selected as down-regulated over the number of total genes included in the GO term.

identified at the time this investigation was initiated: chloroplastic Fe SOD (FSD) 1, FSD2, FSD3, chloroplastic Cu/Zn SOD (CSD) 2, cytoplasmic CSD1, peroxisomal CSD3, and mitochondrial Mn SOD (MSD) (Kliebenstein *et al.*, 1998). As a scavenging enzyme, APX reduces H_2O_2 to H_2O and O_2 via a series of reactions with ascorbic acid. Two isomers, thylakoid-bound APX (tAPX) and stromal APX (sAPX), are known to exist in chloroplasts. Other isomers (APX1–6) are predicted to reside in the cytoplasm or peroxisomes (Shigeoka *et al.*, 2002; Ishikawa and Shigeoka, 2008). Our microarray did indeed indicate that several *SOD* and *APX* genes were up-regulated in *var2* white sectors (see Supplementary Fig. S3 at *JXB* online).

To verify our results from microarray analyses, semi-quantitative RT-PCR was performed first (Fig. 4A). Results showed elevated expression of plastid-localized enzymes, *CSD2* and *sAPX*, although *FSD1* levels appeared to remain unchanged. In addition, the results show that *CCS* (encoding a copper delivery chaperone specific for CSD1 and CSD2) and *CSD1* were up-regulated, suggesting that elevated expression is not limited to chloroplast isoforms. Real-time RT-PCR analysis was performed to quantify the expression levels of *CSD2*, *sAPX*, and *tAPX* (Fig. 4B). Expression levels of *CSD2* and *sAPX* mRNAs were 20.2-fold and 2.8-fold higher in white sectors than in Col, although no significant difference was detectable in *tAPX* expression. None of these genes showed differential expression between Col and *var2* green sectors.

Immunoblot analysis was performed to examine the increased levels of SOD and APX in *var2* white sectors (Fig. 4C). Consistent with mRNA levels, fresh weight-normalized immunoblot analyses indicated that CSD1, CSD2, and sAPX are expressed predominantly in white sectors (Fig. 4C). No detectable level of tAPX, plastocyanin, or LHCII was observed (Fig. 4C), probably because of a lack of thylakoid membranes. Taken together, these results from RT-PCR and immunoblot analyses were consistent with our initial microarray analysis. Therefore, it is concluded that plastidic ROS scavenging enzymes, if not all isoforms, are up-regulated in *var2* white sectors.

Elevated CSD2 expression reflects its enzymatic activity

High levels of SODs in the white sectors, particularly CSD2, prompted us to conduct several additional experiments. In our first experiment, SOD activity was examined

Table 2. Significantly enriched gene ontologies among up-regulated genes in *var2* white sectors compared to *var2* green sectors

Gene ontology (description and term)[a]	Raw *P*	BY-corrected *P*	Number[b]
Cellular component			
Cytoplasm; GO:0005737	0.000	0.012	112/4926
Cytoplasmic part; GO:0044444	0.000	0.012	91/4518
Intracellular non-membrane-bounded organelle; GO:0043232	0.000	0.080	23/784
Mitochondrion; GO:0005739	0.000	0.000	70/991
Non-membrane-bounded organelle; GO:0043228	0.000	0.080	23/784
Ribonucleoprotein complex; GO:0030529	0.000	0.011	24/469
Ribosome; GO:0005840	0.000	0.005	23/370
Biological process			
Biopolymer biosynthetic process; GO:0043284	0.000	0.042	37/860
Gene expression; GO:0010467	0.000	0.000	47/897
ncRNA metabolic process; GO:0034660	0.000	0.002	9/128
ncRNA processing; GO:0034470	0.000	0.002	9/63
Response to chemical stimulus; GO:0042221	0.000	0.030	25/1206
Response to heat; GO:0009408|GO:0006951	**0.000**	**0.002**	**18/114**
Response to hydrogen peroxide; GO:0042542	**0.000**	**0.080**	**9/37**
Response to iron ion; GO:0010039	0.000	0.081	5/9
Response to oxidative stress; GO:0006979	**0.000**	**0.041**	**23/205**
Response to reactive oxygen species; GO:0000302	**0.000**	**0.090**	**10/48**
Response to stimulus; GO:0050896|GO:0051869	0.000	0.001	41/2645
Response to stress; GO:0006950	**0.000**	**0.011**	**39/1558**
Ribosome biogenesis; GO:0042254|GO:0007046	0.000	0.003	17/133
rRNA metabolic process; GO:0016072	0.000	0.001	9/31
rRNA processing; GO:0006364|GO:0006365	0.000	0.001	9/31
Translation; GO:0006412|GO:0006416|GO:0006453|GO:0043037	0.000	0.001	37/545
Molecular function			
Oxidoreductase activity, acting on superoxide radicals as acceptor; GO:0016721	0.000	0.081	5/9
Structural constituent of ribosome; GO:0003735|GO:0003736|GO:0003737|GO:0003738|GO:0003739|GO:0003740|GO:0003741|GO:0003742	0.000	0.007	35/361
Structural molecule activity; GO:0005198	0.000	0.015	37/498
Superoxide dismutase activity; GO:0004784|GO:0004785|GO:0008382|GO:0008383|GO:0016954	**0.000**	**0.081**	**5/9**

[a] GO analysis was performed using a hypergeometric test with GeneSpring GX 10 software. Gene ontology categories are shown with significant Benjamini–Yekutieli FDR (BY–FDR)-corrected *P*-values < 0.1. Gene categories related to stress are shown as bold.
[b] Number indicates the number of genes selected as up-regulated over the number of total genes included in the GO term.

specifically. The CSD and FSD, respectively, require copper/zinc and iron cofactors. Leaf extracts from Col, *var2* green, and *var2* white sectors were subjected to native-PAGE and SOD activities were detected (Fig. 4D). The bands corresponding to CSD, FSD, and MSD were similar to those described in previous reports (Beauchamp and Fridovich, 1971; Kliebenstein *et al.*, 1998). Although this experiment did not distinguish CSD activities from each isomer, it was evident that *var2* white sectors only had significantly high levels of CSD activities (2.1-fold compared to Col). Collectively, these results strongly suggest that cofactors are sufficiently provided in *var2* white sectors and that elevated CSD2 expression reflects its enzymatic activity.

Up-regulation of CSD2 in white sectors is unaffected by cofactor

In our next line of investigation, it was examined whether CSD2 expression is affected by cofactors. Although our findings in *var2* are consistent with the fact that *CSD2* is among the genes induced by oxidative stress, *CSD2* expression is known to be controlled strictly by copper availability (Sunkar *et al.*, 2006; Yamasaki *et al.*, 2007, 2009). Under normal growth conditions, copper is limiting (0.1 μM copper in standard MS medium) (Shikanai *et al.*, 2003; Abdel-Ghany *et al.*, 2005), and FSD1 is expressed predominantly in chloroplasts and CSD2 is repressed. However, under copper-sufficient conditions (5 μM copper), CSD2 expression is enhanced and FSD1 is repressed (Yamasaki *et al.*, 2007). Therefore, there was interest in characterizing the activity and accumulation of plastidic SODs under different copper conditions (Fig. 5A, B). The CSD2 overexpression lines (*CSD2ox*) were examined simultaneously to locate the activity corresponding to CSD2 (Fig. 5B).

Our results show that even under copper-deficient conditions, white sectors exhibited CSD activity as high as that of *CSD2ox*. Immunoblot analysis showed that

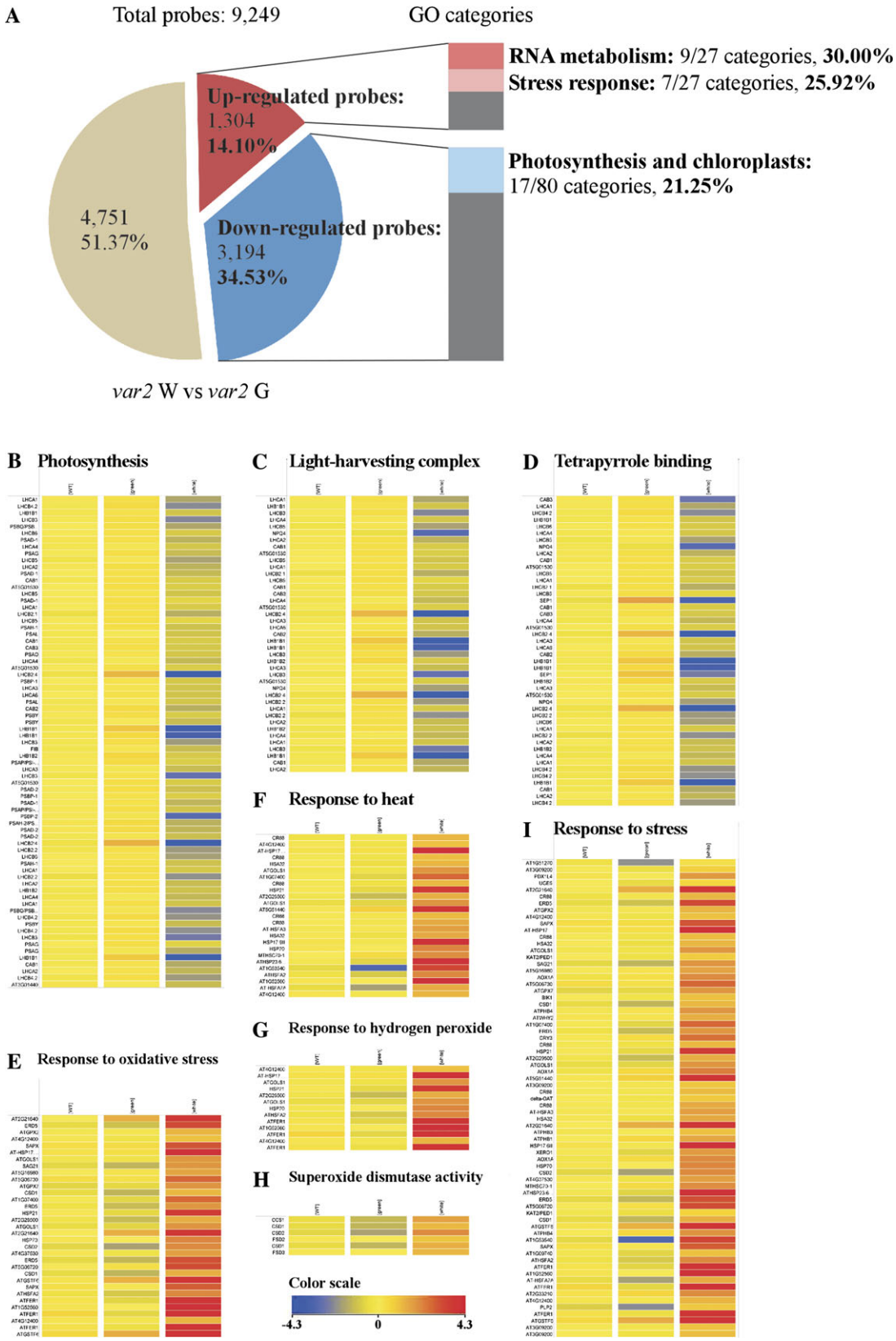

Fig. 3. Microarray expression profile in Columbia and *var2* white/green sectors. (A) A pie graph representation of the rate of up- or down-regulated probes in *var2* white sectors (*var2* W) compared to *var2* green sectors (*var2* G). The rates of each category (RNA metabolism, Stress response and Photosynthesis and chloroplasts) are shown in the bar graph to the right. (B–I) Gene ontology (GO) analysis. Representative categories among down-regulated (B–D) or up-regulated (E–I) genes in *var2* white sectors compared to *var2* green sectors are shown (see Tables 1 and 2). Gene expression profiles according to averaged normalized signal values (see colour scale) in Columbia (WT, left), *var2* green sectors (green, middle), and *var2* white sectors (white, right) are shown as a heat map. Each horizontal bar represents a single gene. (B) Photosynthesis. (C) Light-harvesting complex. (D) Tetrapyrrole binding. (E) Response to oxidative stress. (F) Response to heat. (G) Response to hydrogen peroxide. (H) Superoxide dismutase activity. (I) Response to stress.

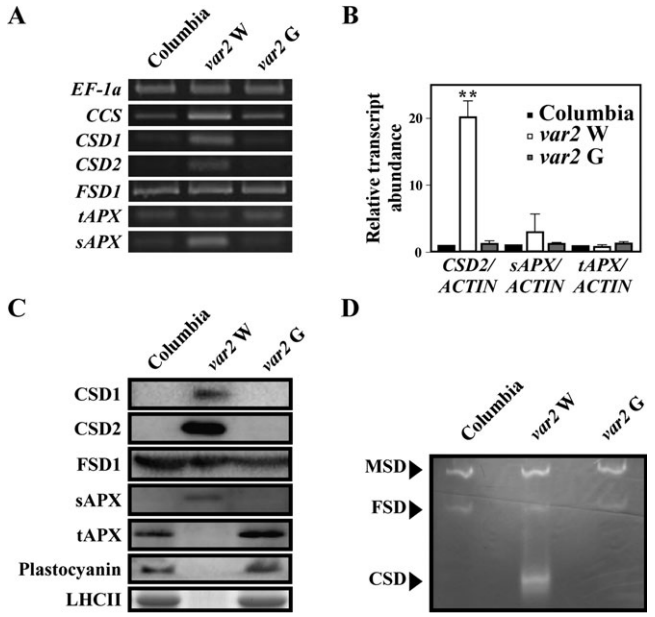

Fig. 4. mRNA and protein levels of ROS scavenging enzymes and SOD activity. (A) Transcript levels in Columbia and *var2* white/green sectors. Semi-quantitative RT-PCR analyses were performed using total RNA from 40-d-old leaves from Columbia, *var2* white (*var2* W) and green (*var2* G) sectors. Expression levels of *CCS*, *CSD1*, *CSD2*, *FSD1*, *tAPX*, and *sAPX* are shown. *EF-1α* was used as an internal control. (B) Quantitative RT-PCR in Columbia and *var2*. Transcript levels of *CSD2*, *sAPX*, and *tAPX* genes from Columbia and *var2* were measured using real-time RT-PCR analysis. *ACTIN* was used as an internal control. Relative ratios of transcript levels compared to Columbia are shown (mean ±SD, n=3). Asterisks denote significant differences from Columbia using Student's t test (** P <0.01). (C) Immunoblot analysis of Columbia and *var2* white (*var2* W) and green (*var2* G) proteins. Immunoblots were normalized based on total fresh weight and were probed with antibodies against CSD2, FSD1, sAPX, tAPX, and plastocyanin (PC). CBB-stained protein bands corresponding to light-harvesting complex II (LHCII) are also shown at the bottom. Because of its ability to cross-react, CSD1 protein levels were detected using the CSD2 antibody. (D) SOD activities. A native gel stained with NBT. SOD activities were measured based on the ability of SOD to inhibit the reduction of NBT by superoxide. Corresponding bands for MSD, FSD, and CSD are shown.

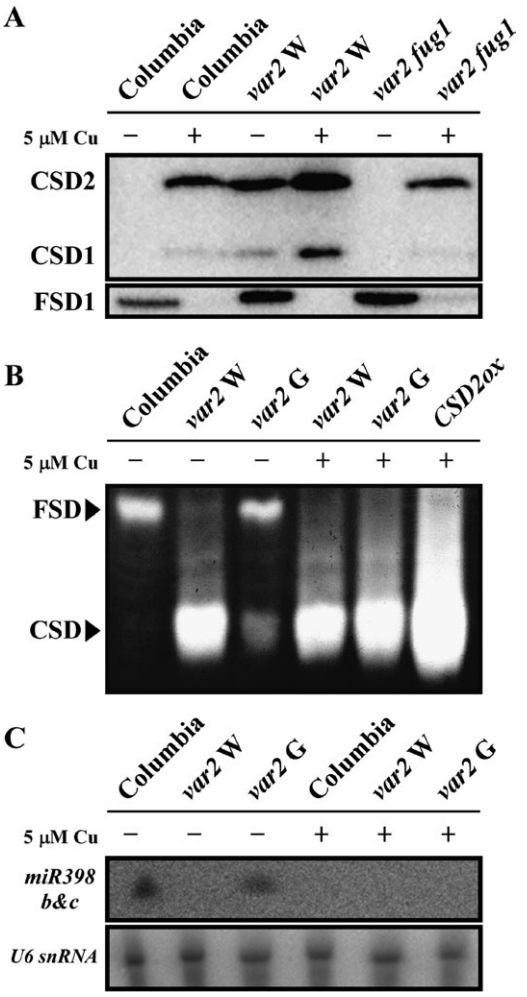

Fig. 5. Effect of copper on CSD accumulation and *miR398* in *var2*. (A) Immunoblot analysis. Proteins from Columbia, white sectors of *var2* (*var2* W), and *var2 fug1* with (+) or without (–) 5 μM $CuSO_4$ were probed with CSD2 and FSD1 antibodies. (B) SOD activities under different copper concentrations. Columbia, *var2*, and *CSD2ox* were subjected to SOD activities with (+) or without (–) 5 μM $CuSO_4$. A native gel is shown as stained with NBT. The SOD activities were measured based on the ability of SOD to inhibit the reduction of NBT by superoxide. Corresponding bands for MSD, FSD, and CSD are shown. (C) RNA blot analysis. Twenty μg of total RNAs from 3-week-old Columbia and *var2* with (+) or without (–) 5 μM $CuSO_4$ were hybridized with probes specific for *miR398 b & c*. *U6 small nuclear RNA* (*U6 snRNA*) was used as a control. Data shown here are representative results from three biological replicates.

although Col and *var2* green sectors responded to copper as reported previously (Yamasaki *et al.*, 2007), white sectors did not; the steady-state level of CSD2 remained (Fig. 5A). By contrast, the levels of accumulation of FSD1 were comparable among Col, *var2* green, and *var2* white sectors (Fig. 4A, C, A), although activity of FSD in *var2* white sectors was lower than Col and *var2* green sectors (Figs 4D, 5B). Up-regulation of CSD2 appeared to be specific to white sectors but not to the *var2* mutation *per se* because a non-variegated suppressor line *var2 fug1* (Miura *et al.*, 2007) showed canonical copper regulation (Fig. 5A).

Up-regulation of CSD2 in white sectors is associated with miR398

It was recently demonstrated that the antagonistic expression of FSD and CSD, which is controlled by copper availability as mentioned earlier, is governed by a microRNA (*miR398*). In fact, *miR398* has been characterized as a key regulatory factor in copper homeostasis (Yamasaki *et al.*, 2007, 2009; Ding and Zhu, 2009) and its target genes include *CSD1*, *CSD2*, and mitochondrial *COX5b-1*

(cytochrome *c* oxidase) (Yamasaki *et al.*, 2007). Therefore RNA blot analysis was performed to examine *miR398* levels (Fig. 5C). Total RNAs prepared from Col, *var2* green and white sectors were hybridized with a probe specific to *miR398b* and *miR398c*. The result confirmed that white sectors did not accumulate any detectable level of *miR398*, irrespective of the copper concentration. Our data therefore demonstrated that *var2* white sectors exhibit up-regulation of plastidic SOD, and that this up-regulation partly results from impaired expression of *miR398*. Differential expression of ROS scavenging enzymes between *var2* green and white sectors therefore appears to result not from photo-oxidative stress but rather from other physiological responses.

Discussion

ROS in var2 *green sectors and transcriptome*

In this study, it was examined if significant levels of ROS in *var2* green sectors, suffered from photo-oxidative stress, result in up-regulation of ROS signalling and/or scavenging. In plants, the main cellular compartments for ROS production are chloroplasts (plastids), mitochondria, and peroxisomes (Mittler, 2002; Apel and Hirt, 2004; Foyer and Noctor, 2005). Each compartment has its own scavenging enzymes to detoxify excess ROS, which otherwise oxidize and damage proteins, lipids, and nucleic acids. Such damage might ultimately affect plant growth adversely. On the other hand, ROS at non-lethal levels act as a signalling molecule and influence many stress responses such as high light, salinity, high or low temperature, and heavy metals (Mittler, 2002; Apel and Hirt, 2004; Foyer and Noctor, 2005). The involvement of chloroplastic ROS as a signalling molecule was previously implicated (Joo *et al.*, 2005). In fact, ROS scavenging enzymes are induced to decrease toxic ROS generated mainly in chloroplasts and mitochondria during abiotic stresses (Apel and Hirt, 2004). At the time of biotic stress, ROS scavenging systems are rather suppressed and ROS are enhanced by enzymatic activity of plasma-membrane-bound NADPH oxidases to induce the onset of programmed cell death, including the expression of defence-related genes (Apel and Hirt, 2004). In contrast to these observations, however, our scatter plot, GO, and metabolic pathway analyses revealed none of these responses in *var2* green sectors. It is hypothesized that ROS in *var2* is not at a sufficiently high level to activate the signalling pathway and/or ROS in chloroplasts do not directly affect the ROS signalling pathway. Alternatively, ROS signalling might be inhibited specifically by a FtsH defect in the *var2* green sectors.

Down-regulation of photosynthetic genes in white sectors

A main objective of this study was to elucidate the overall transcriptional profile in the *Arabidopsis* variegated mutant *var2*. Comparative microarray analyses from dissected green and white leaf sectors identified numerous activated or repressed genes. Aluru *et al.* (2009) recently reported a similar result from a comparative analysis of variegated sectors from the *im* mutant. In both *im* and *var2* mutants, the genes for the light reactions of photosynthesis, including Photosystems, Light harvesting complex, and Tetrapyrrole biosynthesis, were repressed strongly in the white sectors (Aluru *et al.*, 2009). These results accord well with the fact that cells in the white sectors of these variegated mutants are devoid of thylakoid membranes. Consequently, it is likely that the irreversible repression of the photosynthetic genes described above forms white sectors, irrespective of the type of original mutation. Different mutations responsible for variegation contribute to the pattern of leaf variegation: variegations in *im, var2*, and *chloroplast mutator* are mutually indistinguishable (Sakamoto, 2003).

Up-regulation of oxidative and other stress-related genes in white sectors

A considerable number of genes (14%) exhibited more than a 2-fold transcript increase in white sectors (Fig. 3A). The GO analysis revealed two classes of GO categories that are remarkably activated in *var2* white sectors. One category is RNA metabolism, including Ribosomes, Ribonucleoprotein complexes, ncRNA metabolic processing, and rRNA metabolic processing (Table 1). The *Arabidopsis* microarray (ver. 4; Agilent Technologies Inc.) that was used for this study also contained chloroplast genes. It is particularly interesting that transcripts for numerous ribosomal genes in chloroplasts (e.g. *RPL20*, *RPS15*) increased in *var2* white sectors (data not shown). The precise reason for this up-regulation is currently unclear.

Activation for the other GO category, which contained stress-related genes, is also noteworthy. For example, numerous heat-shock proteins such as HSP70 were highly up-regulated in white sectors (Fig. 3I; see Supplementary Table S1 available at *JXB* online). The HSPs not only aid in the protection of proteins from heat and other stresses, they also play a pivotal role in protein folding along with enhanced protein synthesis (Zhang and Glaser, 2002). Specific heat shock factors such as *HsfA2* that are up-regulated in white sectors (Fig. 3I; see Supplementary Table S1 at *JXB* online), function as molecular sensors that sense ROS directly and regulate stress responses (Davletova *et al.*, 2005; Miller and Mittler, 2006). Furthermore, glutathione peroxidases (GPX) are key enzymes of the antioxidant networks in both plants and animals. Two glutathione peroxidases (*ATGPX2* and *ATGPX7*) were up-regulated in white sectors (Fig. 3I; see Supplementary Table S1 at *JXB* online). Recent evidence indicates the importance of chloroplast-localized AtGPX7 for the regulation of cellular photo-oxidative tolerance and immune responses (Chang *et al.*, 2009). Consequently, it is apparent that white sectors respond to impaired plastid development and mitigate their susceptibility by activating various stress genes.

Response to oxidative stress in white sectors

It was initially hypothesized that *var2* white sectors receive photo-oxidative stress at levels less than that that green sectors experience. It is noteworthy, however, that CSD2 up-regulation is limited to white sectors, despite the fact that green sectors accumulate high levels of ROS. Because plastids in white sectors are almost devoid of thylakoids and photosystems, white sectors might experience oxidative stress of a different type that does not result from the photoinhibition of PSII. For example, DNA oxidation, lipid peroxidation, and protein oxidation occur during several metabolic processes in organelles without thylakoids and photosystems. Moreover, because leaf tissues are originally subjected to light, several precursors of photosynthesis-related proteins might be fed into plastids of *var2* white sectors similar to chloroplasts. Supporting these possibilities, the plastids of white *albostrians* leaves retain the ability to synthesize tetrapyrroles halfway (Yaronskaya *et al.*, 2003). Some of these biosynthetic intermediate precursors (such as protochlorophyllide) might cause photo-oxidative damage in plastids (Meskauskiene *et al.*, 2001). Further study is necessary to elucidate the physiological properties of *var2* white sectors.

CSD2 up-regulation implicates stress response common in white sectors

Similarly to the down-regulated genes, the up-regulated genes in white sectors were shared in *var2* and *im* (Aluru *et al.*, 2009). This observation raises a possibility that tissues containing aberrant plastids (e.g. albino plants) as well as variegated sectors respond to oxidative stress. A literature search revealed that CSD2 is up-regulated in several *Arabidopsis* albino mutants (*fsd2*, *fsd3*, *tic21 pic1-1*, *tic20*, *alb3*, and *emb1303-1*, Myouga *et al.*, 2008; Huang *et al.*, 2009; Kikuchi *et al.*, 2009). In addition to these observations, CSD2 expression was examined in non-green tissues such as roots and calli that contain amyloplasts (see Supplementary Fig. S4 at *JXB* online). No induction of CSD2 protein or activity was detectable in these tissues. These results together imply that up-regulation of genes related to oxidative stress is a general response of tissues that contain defective chloroplast development. Overexpression of CSD2 apparently has no effect on the formation of leaf variegation (E Miura, unpublished data). Differential expression of CSD2 between white and green sectors does not simply contribute to the formation of leaf variegation. Although our transcriptome analysis demonstrates a physiological state of white sectors, it remains unclear how variegated sectors are formed. Further study on that subject is necessary.

One interesting finding of this study is the sector-specific accumulation of a microRNA, *miR398*, which negatively regulates *CSD2* expression by acting as a sensor component for copper availability. Chloroplasts are a major reservoir for copper because of the presence of plastocyanin, which is an electron transporter between cytochrome *b6/f* and PSI. Although copper functions as a necessary cofactor for plastocyanin, excess free copper might cause oxidative stress and cytotoxicity (Luna *et al.*, 1994; Zhang *et al.*, 2008). Although further investigation is necessary, two inferences can be drawn from the repression of *miR398* in *var2* white sectors. First, CSD2 up-regulation is partly caused by copper availability and is a result of copper homeostasis rather than ROS scavenging. White sectors apparently lack thylakoids and plastocyanin, which can mimic a copper-sufficient condition. Second, white sectors are necessary to control strictly free transition metals (e.g. Cu and Fe) for protection from oxidative stress. For example, accumulation of FSD in white sectors is also explained by the lack of the Reiske Fe-S protein in cytochrome *b6/f*, which requires iron as a cofactor. Supporting this possibility is the up-regulation of ferritin (FER), which was previously found to function as an iron buffer and which is induced in response to oxidative stress (Petit *et al.*, 2001; Briat *et al.*, 2009). When our microarray data were re-examined for *FER* genes (*AtFER1, 3,* and *4*), results showed that these genes were up-regulated in white sectors (see Supplementary Fig. S5 at *JXB* online). Consequently, our study in SOD again shows a common response to oxidative stress in the variegated sectors.

Conclusion

In *var2*, both green and whites sectors are produced by living cells. However, physiological properties of both sectors differ profoundly. Green sectors suffer from photo-oxidative stress because of impaired PSII repair, and white sectors receive various oxidative stresses because of aberrant chloroplast development. Although *var2* green sectors, which produce ROS in chloroplasts, do not display detectable responses to ROS signalling and scavenging, white sectors do respond to the stresses and activate many genes such as *CSD2* and *sAPX*. The activation of stress-related genes is found in tissues with aberrant chloroplast differentiation as well as in variegated white sectors, probably as a common response to protect defective tissues that result from mutation.

Supplementary data

The following supplementary data are available at *JXB* online:

Supplementary Fig. S1. Venn diagram of differentially regulated genes in *var2*.

Supplementary Fig. S2. Bird's eye map by KaPPA-View.

Supplementary Fig. S3. Expression levels of *CCS*, *SOD* and *APX* genes.

Supplementary Fig. S4. SOD accumulation and activity in *var2* roots and callus.

Supplementary Fig. S5. Expression levels of *Ferritin* genes.

Supplementary Table S1. Gene lists of Fig. 3B–I.

Supplementary Table S2. Primers used for RT-PCR and real-time RT-PCR.

Acknowledgements

The authors would like to thank Dr S Shigeoka (Kinki University) for sAPX and tAPX antibodies, Dr T Shikanai (Kyoto University) for FSD and plastocyanin antibodies, *Arabidopsis* CSD2ox-2 (*CSD2ox*), Dr K Goto (Okayama Research Institute of Biological Institute) for help with GeneSpring GX 10 software, and Dr K Rikiishi (Okayama University) for help with real-time RT-PCR analysis. This work was supported by a Grant-in-Aid for Scientific Research from the Ministry of Education, Culture, Sports, Science, and Technology (MEXT) (16085207 and 19657017), the Asahi Glass Foundation, and the Oohara Foundation. EM is supported by a postdoctoral fellowship from the Japan Society for the Promotion of Science (JSPS).

References

Abdel-Ghany SE, Müller-Moulé P, Niyogi KK, Pilon M, Shikanai T. 2005. Two P-type ATPases are required for copper delivery in *Arabidopsis thaliana* chloroplasts. *The Plant Cell* **17,** 1233–1251.

Abdel-Ghany SE, Pilon M. 2008. MicroRNA-mediated systemic down-regulation of copper protein expression in response to low copper availability in *Arabidopsis*. *Journal of Biological Chemistry* **283,** 15932–15945.

Adam Z, Rudella A, van Wijk KJ. 2006. Recent advances in the study of Clp, FtsH and other proteases located in chloroplasts. *Current Opinion in Plant Biology* **9,** 234–240.

Aluru MR, Stessman DJ, Spalding MH, Rodermel SR. 2007. Alterations in photosynthesis in *Arabidopsis* lacking IMMUTANS, a chloroplast terminal oxidase. *Photosynthesis Research* **91,** 11–23.

Aluru MR, Zola J, Foudree A, Rodermel SR. 2009. Chloroplast photo-oxidation-induced transcriptome reprogramming in *Arabidopsis immutans* white leaf sectors. *Plant Physiology* **150,** 904–923.

Apel K, Hirt H. 2004. Reactive oxygen species: metabolism, oxidative stress, and signal transduction. *Annual Review of Plant Biology* **55,** 373–399.

Asada K. 2006. Production and scavenging of reactive oxygen species in chloroplasts and their functions. *Plant Physiology* **141,** 391–396.

Ashburner M, Ball CA, Blake JA, *et al*. 2000. Gene ontology: tool for the unification of biology. *Nature Genetics* **25,** 25–29.

Bailey S, Thompson E, Nixon PJ, Horton P, Mullineaux CW, Robinson C, Mann NH. 2002. A critical role for the Var2 FtsH homologue of *Arabidopsis thaliana* in the photosystem II repair cycle *in vivo*. *Journal of Biological Chemistry* **277,** 2006–2011.

Beauchamp C, Fridovich I. 1971. Superoxide dismutase: improved assays and an assay applicable to acrylamide gels. *Analytical Biochemistry* **44,** 276–287.

Briat JF, Ravet K, Arnaud N, Duc C, Boucherez J, Touraine B, Cellier F, Gaymard F. 2009. New insights into ferritin synthesis and function highlight a link between iron homeostasis and oxidative stress in plants. *Annals of Botany* 10.1093/aob/mcp128.

Chang CC, Ślesak I, Jordá L, Sotnikov A, Melzer M, Miszalski Z, Mullineaux PM, Parker JE, Karpińska B, Karpiński S. 2009. Arabidopsis chloroplastic glutathione peroxidases play a role in cross talk between photo-oxidative stress and immune responses. *Plant Physiology* **150,** 670–683.

Chen M, Choi Y, Voytas DF, Rodermel S. 2000. Mutations in the Arabidopsis *VAR2* locus cause leaf variegation due to the loss of a chloroplast FtsH protease. *The Plant Journal* **22,** 303–313.

Davletova S, Rizhsky L, Liang H, Shengqiang Z, Oliver DJ, Coutu J, Shulaev V, Schlauch K, Mittler R. 2005. Cytosolic ascorbate peroxidase 1 is a central component of the reactive oxygen gene network of Arabidopsis. *The Plant Cell* **17,** 268–281.

Ding YF, Zhu C. 2009. The role of microRNAs in copper and cadmium homeostasis. *Biochemical and Biophysical Research Communications* **386,** 6–10.

Foyer CH, Noctor G. 2005. Redox homeostasis and antioxidant signalling: a metabolic interface between stress perception and physiological responses. *The Plant Cell* **17,** 1866–1875.

Huang X, Zhang X, Yang S. 2009. A novel chloroplast-localized protein EMB1303 is required for chloroplast development in *Arabidopsis*. *Cell Research* **19,** 1205–1216.

Ishikawa T, Shigeoka S. 2008. Recent advances in ascorbate biosynthesis and the physiological significance of ascorbate peroxidase in photosynthesizing organisms. *Bioscience, Biotechnology, and Biochemistry* **72,** 1143–1154.

Joo JH, Wang S, Chen JG, Jones AM, Fedoroff NV. 2005. Different signalling and cell death roles of heterotrimeric G protein alpha and beta subunits in the Arabidopsis oxidative stress response to ozone. *The Plant Cell* **17,** 957–970.

Kato Y, Miura E, Matsushima R, Sakamoto W. 2007. White leaf sectors in *yellow variegated2* are formed by viable cells with undifferentiated plastids. *Plant Physiology* **144,** 952–960.

Kato Y, Miura E, Ido K, Ifuku K, Sakamoto W. 2009. The variegated mutants lacking chloroplastic FtsHs are defective in D1 degradation and accumulate reactive oxygen species. *Plant Physiology* **151,** 1790–1801.

Kato Y, Sakamoto W. 2009. Protein quality control in chloroplasts: a current model of D1 protein degradation in the photosystem II repair cycle. *Journal of Biochemistry* **146,** 463–469.

Kikuchi S, Oishi M, Hirabayashi Y, Lee DW, Hwang I, Nakai M. 2009. A 1-megadalton translocation complex containing Tic20 and Tic21 mediates chloroplast protein import at the inner envelope membrane. *The Plant Cell* **21,** 1781–1797.

Kliebenstein DJ, Monde RA, Last RL. 1998. Superoxide dismutase in Arabidopsis: an eclectic enzyme family with disparate regulation and protein localization. *Plant Physiology* **118,** 637–650.

Luna CM, González CA, Trippi VS. 1994. Oxidative damage caused by excess of copper in oat leaves. *Plant and Cell Physiology* **35,** 11–15.

Meskauskiene R, Nater M, Goslings D, Kessler F, op den Camp R, Apel K. 2001. FLU: a negative regulator of chlorophyll biosynthesis in *Arabidopsis thaliana*. *Proceedings of the National Academy of Sciences, USA* **98,** 12826–12831.

Miller G, Mittler R. 2006. Could heat shock transcription factors function as hydrogen peroxide sensors in plants? *Annals of Botany* **98,** 279–288.

Mittler R. 2002. Oxidative stress, antioxidants and stress tolerance. *Trends in Plant Science* **7,** 405–410.

Miura E, Kato Y, Matsushima R, Albrecht V, Laalami S, Sakamoto W. 2007. The balance between protein synthesis and degradation in chloroplasts determines leaf variegation in *Arabidopsis yellow variegated* mutants. *The Plant Cell* **19,** 1313–1328.

Myouga F, Hosoda C, Umezawa T, Iizumi H, Kuromori T, Motohashi R, Shono Y, Nagata N, Ikeuchi M, Shinozaki K. 2008. A heterocomplex of iron superoxide dismutases defends chloroplast nucleoids against oxidative stress and is essential for chloroplast development in *Arabidopsis*. *The Plant Cell* **20,** 3148–3162.

Nixon PJ, Barker M, Boehm M, de Vries R, Komenda J. 2005. FtsH-mediated repair of the photosystem II complex in response to light stress. *Journal of Experimental Botany* **56,** 357–363.

Petit JM, Briat JF, Lobreaux S. 2001. Structure and differential expression of the four members of the *Arabidopsis thaliana ferritin* gene family. *Biochemical Journal* **359,** 575–582.

Sakamoto W, Tamura T, Hanba-Tomita Y, Murata M. 2002. The *VAR1* locus of *Arabidopsis* encodes a chloroplastic FtsH and is responsible for leaf variegation in the mutant alleles. *Genes to Cells* **7,** 769–780.

Sakamoto W. 2003. Leaf-variegated mutations and their responsible genes in *Arabidopsis thaliana*. *Genes and Genetic Systems* **78,** 1–9.

Sakamoto W, Zaltsman A, Adam Z, Takahashi Y. 2003. Coordinated regulation and complex formation of YELLOW VARIEGATED1 and YELLOW VARIEGATED2, chloroplastic FtsH metalloproteases involved in the repair cycle of photosystem II in Arabidopsis thylakoid membranes. *The Plant Cell* **15,** 2843–2855.

Sakamoto W. 2006. Protein degradation machineries in plastids. *Annual Review of Plant Biology* **57,** 599–621.

Sakamoto W, Uno Y, Zhang Q, Miura E, Kato Y, Sodmergen. 2009. Arrested differentiation of proplastids into chloroplasts in variegated leaves characterized by plastid ultrastructure and nucleoid morphology. *Plant and Cell Physiology* **50,** 2069–2083.

Shigeoka S, Ishikawa T, Tamoi M, Miyagawa Y, Takeda T, Yabuta Y, Yoshimura K. 2002. Regulation and function of ascorbate peroxidase isoenzymes. *Journal of Experimental Botany* **53,** 1305–1319.

Shikanai T, Müller-Moulé P, Munekage Y, Niyogi KK, Pilon M. 2003. PAA1, a P-type ATPase of Arabidopsis, functions in copper transport in chloroplasts. *The Plant Cell* **15,** 1333–1346.

Sunkar R, Kapoor A, Zhu JK. 2006. Posttranscriptional induction of two *Cu/Zn superoxide dismutase* genes in *Arabidopsis* is mediated by downregulation of *miR398* and important for oxidative stress tolerance. *The Plant Cell* **18,** 2051–2065.

Takechi K, Sodmergen Murata M, Motoyoshi F, Sakamoto W. 2000. The *YELLOW VARIEGATED* (*VAR2*) locus encodes a homologue of FtsH, an ATP-dependent protease in *Arabidopsis*. *Plant and Cell Physiology* **41,** 1334–1346.

Tokimatsu T, Sakurai N, Suzuki H, Ohta H, Nishitani K, Koyama T, Umezawa T, Misawa N, Saito K, Shibata D. 2005. KaPPA-view: a web-based analysis tool for integration of transcript and metabolite data on plant metabolic pathway maps. *Plant Physiology* **138,** 1289–1300.

Von Wirén N, Mori S, Marschner H, Römheld V. 1994. Iron inefficiency in maize mutant *ys1* (*Zea mays* L. cv. yellow-stripe) is due to a defect in uptake of iron phytosiderophores. *Plant Physiology* **106,** 71–77.

Yamasaki H, Abdel-Ghany SE, Cohu CM, Kobayashi Y, Shikanai T, Pilon M. 2007. Regulation of copper homeostasis by micro-RNA in *Arabidopsis*. *Journal of Biological Chemistry* **282,** 16369–16378.

Yamasaki H, Hayashi M, Fukazawa M, Kobayashi Y, Shikanai T. 2009. SQUAMOSA promoter binding protein-like7 is a central regulator for copper homeostasis in *Arabidopsis*. *The Plant Cell* **21,** 347–361.

Yaronskaya E, Ziemann V, Walter G, Averina N, Börner T, Grimm B. 2003. Metabolic control of the tetrapyrrole biosynthetic pathway for porphyrin distribution in the barley mutant *albostrians*. *The Plant Journal* **35,** 512–522.

Yu F, Liu X, Alsheikh M, Park S, Rodermel S. 2008. Mutations in *SUPPRESSOR OF VARIEGATION1*, a factor required for normal chloroplast translation, suppress *var2*-mediated leaf variegation in Arabidopsis. *The Plant Cell* **20,** 1786–1804.

Zaltsman A, Ori N, Adam Z. 2005. Two types of FtsH protease subunits are required for chloroplast biogenesis and Photosystem II *repair in Arabidopsis*. *The Plant Cell* **17,** 2782–2790.

Zhang H, Xia Y, Wang G, Shen Z. 2008. Excess copper induces accumulation of hydrogen peroxide and increases lipid peroxidation and total activity of copper-zinc superoxide dismutase in roots of *Elsholtzia haichowensis*. *Planta* **227,** 465–475.

Zhang XP, Glaser E. 2002. Interaction of plant mitochondrial and chloroplast signal peptides with the Hsp70 molecular chaperone. *Trends in Plant Science* **7,** 14–21.